Lignin oxidation by MnO2 under the irradiation of blue light

Journal:	*Green Chemistry*
Manuscript ID	GC-ART-11-2018-003498.R3
Article Type:	Paper
Date Submitted by the Author:	25-Feb-2019
Complete List of Authors:	Dai, Jinhuo; Monash University, School of Chemistry Patti, Antonio; Monash University, School of Chemistry Styles, Gavin; Monash University, School of Chemistry Nanayakkara, Sepa; Monash University, Centre for Green Chemistry Spiccia, Leone; Monash University, School of Chemistry Arena, Francesco; University of Messina, Engineering Italiano, Cristina ; CNR Institute of Advanced Technology for Energy "Nicola Giordano" Saito, Kei; Monash University, Centre for Green Chemistry, School of Chemistry

Journal Name

ARTICLE

Lignin oxidation by MnO_2 under the irradiation of blue light

Jinhuo Dai,[a§] Antonio F. Patti,[a*] Gavin N. Styles,[a§] Sepa Nanayakkara,[a] Leone Spiccia,[a] Francesco Arena,[b] Cristina Italiano,[c] Kei Saito[a*]

Received 00th January 20xx,
Accepted 00th January 20xx

DOI: 10.1039/x0xx00000x

www.rsc.org/

Traditionally, conventional heat has been required for a large proportion of the oxidation and degradation process to utilise lignin from biomass. A photocatalysis system which is considered as a novel and green strategy for chemical reactions has been applied and photo-MnO_2 catalytic lignin oxidation method has been developed. In this study, we investigated a promising photocatalytic heterogeneous system for lignin oxidation. Recyclable MnO_2 which is readily available, and blue light which is harzardless light are used in this system. 1-Phenylethanol was used as a model compound to study the suitable conditions for this system. After optimizing the reaction conditions, organosolv lignin, kraft lignin, and alkali lignin were applied to this system and showed the successful oxidation of lignins and further degradation.

Introduction

In recent decades, with the increasing demand of renewable materials for chemical feedstock all around the world, lignocellulosic biomass, including lignin, cellulose and hemicellulose, have attracted much attention due to the abundant reserve from nature. Cellulose has been widely used in the paper and pulp industry; however, lignin is still a by-product and considered as a waste existing in the black liquor from some paper making processes.[1-5] The most common way to utilize this "waste" is burn it to supply energy for the process. Lignin is the most abundant renewable source of aromatic units, and has the potential to be used in the production of phenolic compounds as well as bio-based polymers.[6,7] The challenge for lignin depolymerisation is always that there is no defined structure for lignin; however, it is well known that there are several typical linkages in lignin including β-O-4, 4-O-5, 5-5, β-β, and α-O-4 bonds.[3, 7-9]

Of these, the β-O-4 linkage, which contains primary alcohol at the C_γ position and a secondary alcohol at the C_α position, is the most abundant in most types of lignin (Fig. 1).[7-10] Research carried out by Constant et al.[12] and Crestini et al.[13] demonstrated that the technical lignins, such as kraft lignin, soda lignin and wheat straw organosolv lignin, showed

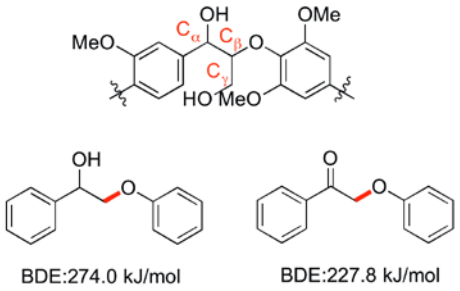

Fig. 1: β-O-4 linkages in lignin

different linkage composition compare to other lignin samples. Particularly, the percentage of β-O-4 bonds decreased due to the lignin degradation that occurred during the industrial process. Das et al.[14] investigated formic-acid-induced hydrolytic lignin oxidation and depolymerisation with different lignin samples. Their results showed that their system can depolymerise all lignin including native lignin. The laboratory isolated lignin, which had higher β-O-4 bonds content than native lignin was used to demonstrate more efficient depolymerisation and to prove their mechanism of β-O-4 bonds cleavage. It has been reported that the oxidation of the secondary benzylic alcohol into a ketone promotes the depolymerisation of most lignin via the cleavage of β-O-4 linkages.[1, 8-15]

The bond dissociation energy of the C-OPh bond is decreased after oxidation (Fig.1).[7-10] Thus, this selective lignin oxidation has a significant role in the process of lignin utilization. Numerous strategies have been reported for the degradation of lignin into smaller molecules after the oxidation of β-O-4 linkages. Rahimi et al.[16], Ma et al.[17] and Lancefield et al.[18] have reported methods using TEMPO/O_2, TEMPO/$Fe(NO_3)_3$, and DDQ(2.3-dichloro-5,6-dicyano-1,4 benzoquinone)/*t*BuONO/O_2 systems for the oxidation of β-O-4

[a] *School of Chemistry, Monash University, Wellington Rd., Clayton, 3800, Victoria, Australia*
[b] *Dipartimento di Ingegneria Elettronica, Chimica e Ingegneria Industriale, Università degli Studi di Messina, I-98166 Messina, Italy*
[c] *CNR Institute of Advanced Technology for Energy "Nicola Giordano", Via Salita S. Lucia 5, 98126 Messina, Italy*
§ These authors contributed equally to this research work
§Electronic Supplementary Information (ESI) available: [details of any supplementary information available should be included here]. See DOI: 10.1039/x0xx00000x

bonds in lignin. These strategies can selectively oxidise the secondary alcohol in β-O-4 bonds in lignin into ketones. However, conventional heating is always required for all the reactions. With the consideration of using renewable and pollution-free energy, photo-catalysis has now presented itself as a preferable choice for benzilic alcohol oxidation over these conventional treatments, as it can utilize solar energy.[19-21]

Photo-catalysis has been widely used in different research areas. It was originally applied for the decomposition of water into hydrogen and oxygen by using a TiO_2 photo-anode in 1972.[22] Since then, the basic mechanisms of photo-catalysis have been studied and published by numerous research groups.[20-27]

Photo-catalysis has also been introduced into lignin chemistry to depolymerise lignin.[25] Nguyen et al.[27] developed a lignin depolymerisation approach using ([4-AcNH-TEMPO]BF_4) as a recyclable oxidant with a photo catalyst. The C–O bond could be cleaved by utilizing the photo-catalyst $[Ir(ppy)_2(dtbbpy)]PF_6$ to selectively oxidise the secondary alcohol to a ketone in β-O-4 model compounds. Tanaka et al.[28] reported that in a lignin solution with suspended TiO_2, lignin was first adsorbed onto the surface of the TiO_2, which was then irradiated by UV (λ>310nm). Lignin was then desorbed and depolymerised with the subsequent illumination. However, carboxylic acids and aldehydes were detected as products due to the aromatic ring opening during the reaction, which indicates that this system cannot be used to generate phenolic compounds from lignin. Ksibi et al.[29] reported the photo-degradation of soluble lignin from black liquor using a UV/TiO_2 photo-catalytic technique. The reaction was carried out at a temperature of 20°C under the irradiation of UV (λ>290nm). Products including vanillin, coniferylic alcohol, syringaldehyde, vanillic acid, were detected by GC-MS. Machado et al.[30] reported a combination of TiO_2 and H_2O_2 with oxygen bubbling under the irradiation of UV/visible light. In their study, the degradation of phenolic groups occurred by electron transfer between the phenolate anion and the ground state oxygen. The hydroxylation of the lignin aromatic structure was also reported.

TiO_2 is generally considered to be an excellent photo-catalyst for lignin oxidation. However, it should be noted that only the ultraviolet light photons, which account for only 4% of solar radiation, can replace its valence band electrons due to a band-gap energy of 3.2eV.[27] Unsurprisingly, as the field has developed, a large range of new and efficient catalysts have emerged in the quest for high energy yield efficiency.[31-35]

MnO_x catalysts and doped analogues have also been extensively studied and applied in water treatment specifically to oxidise and remove organic pollutants. Under milder conditions, selective oxidation has also been reported. The selective oxidation of alcohols to the corresponding carbonyl compounds has been known for some time and widely used in industrial reactions.[36-37] Many studies on the selective aerobic oxidation of benzyl alcohol to benzaldehyde have involved the use of MnO_x materials including combinations that incorporate a variety of promoters and dopants that improve redox behaviour.[38]

MnO_2 is known to exist in a wide variety of structural forms and these forms have a significant bearing on the photo-catalytic behaviour of these materials.[34] These often contain significant amounts of other ions as incorporated into their structure. These structures are composed of a manganese metal centre with oxygens coordinated in an octahedral geometry.[40]

The most commonly used form, γ-MnO_2 is generally found in the cathode material of dry-cell batteries. However, the most active catalytic form for the oxidation of alcohols is reported to be δ-MnO_2. It has a layered structure, with sheets made from manganese-oxygen octahedra, separated by alkali or other ions, and water.[39] Gritter et al. [38] also studied the oxidation of allylic alcohols and benzyl alcohols, in which several forms of manganese oxide were investigated in the oxidation of such alcohols. Zhou et al.[39-41] studied the catalytic ability of MnO_2 for water splitting in the wavelength range from 370 nm to 570 nm, covering a significant part of the visible spectrum.

The application of visible light in the presence of MnO_2 for the selective oxidation of a broader range of alcohols has received little attention, particularly from the perspective of synthetic organic chemistry and controlled transformations. Consequently, the aim of this study was to explore the effect of blue light on the oxidation of benzilic alcohols with a focus on the δ-MnO_2 form. Three other forms of MnO_2 (α, β, γ) were also prepared by reported methods[44] and first tested against a reference model compound, 1-phenylethanol. The different forms of MnO_2 can be readily characterized by X-ray diffraction and were compared with published spectra reported by Villalobos et al.[45] The X-ray diffraction spectrum of the δ-MnO_2 sample is shown in Figure 2.

Herein, we present a very efficient lignin oxidation approach using δ-MnO_2 as a photo-catalyst under the irradiation of blue light (λ = 470 nm) with oxygen bubbling through. 1-phenylethanol and a range of other alcohols, including lignin model compounds, were used to test this catalyst system. After optimising the reaction conditions, original lignin samples were also tested using the same system.

Results and discussion

Characterisation of δ-MnO_2

Synthesized MnO_2 was characterised using XRD, N_2-physisorption and temperature programmed reduction (H_2-TPR) tests to confirm its form and analyse its surface area and particle diameter. The XRD pattern of the synthesized MnO_2 sample (Fig. 2) shows four main reflections at ca. 12°, 25°, 37° and 66.5° (indexed to JCPDS 80-1098), which are typical of the δ-MnO_2 phase.[45]

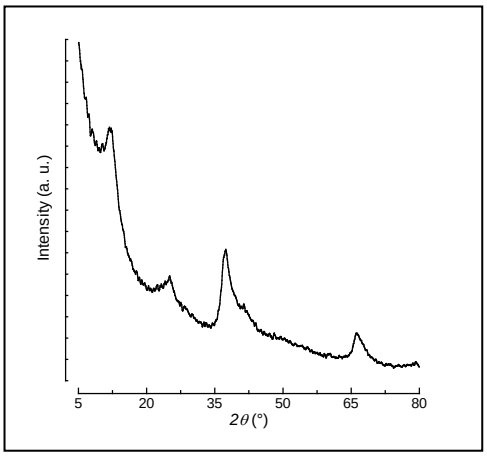

Fig.2: XRD pattern of the δ-MnO_2 sample

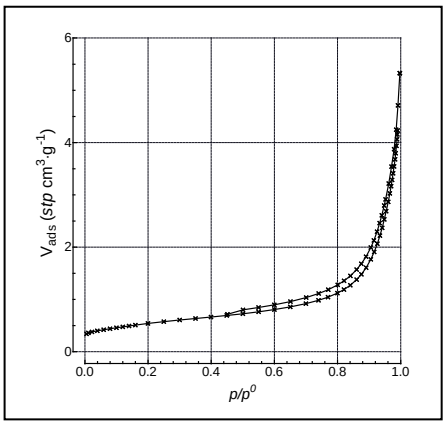

Fig. 3: N_2-physical adsorption isotherm of δ-MnO_2 sample.

The δ-MnO_2 sample featured a N_2-physisorption isotherm typical of macroporous solids, accounting for a Brunauer–Emmett–Teller (BET) surface area value of 43±2 m^2/g (Fig.3). Accordingly, a rather featureless desorption branch indicated an intra-particle porosity of 0.18 cm^3/g, and an average pore diameter of 18 nm. The particle size of δ-MnO_2 was ca. 4 μm, which was analysed by the optical microscope (Fig.S14). For the following reactions, ca. 5-hold excess of MnO_2 was applied to carry out the catalytic reaction from these results.

The H_2-TPR profile of the δ-MnO_2 material, shown in Fig. 4 shows two reduction peaks at 335 and 376°C, respectively, indicating a considerably harder reducibility in comparison to poorly crystalline MnO_2 samples.[47] The overall consumption corresponds to a H_2/Mn ratio of 0.9±0.05, in agreement with the final reduction of the MnO_2 material (i.e., $MnO_{1.9\pm0.05}$) to MnO, while the relative intensity of the reduction peaks suggests the intermediate formation or presence of Mn_2O_3 species. In a separate study of manganese oxide molecular sieves, Tang et al.[48] included a H_2-TPR of their material and suggested that the lower temperature reduction peak may be associated with the reduction of MnO_2–Mn_3O_4, while the higher temperature peak is associated with further reduction of Mn_3O_4 to MnO. As a result, the synthesized MnO_2 was confirmed as δ-MnO_2.

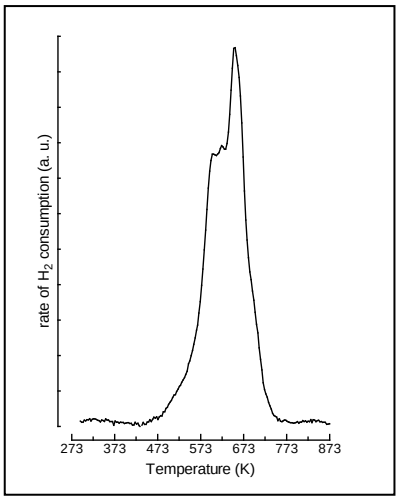

Fig. 4: H_2-TPR of the δ-MnO_2 sample.

Oxidation reactions of alcohols

In order to establish optimum conditions for this photo-catalysis system, 1-phenylethanol was used as a model compound. ^{1}H-NMR was used to confirm the conversion of 1-phenylethanol to acetophenone by comparing the signals for the terminal methyl group of both compounds, which showed a doublet around 1.41 ppm for 1-phenylethanol and a singlet at 2.59 ppm for the oxidation product (Supporting Information Fig. S1, Fig. S3). The recovered mass yield of reacted products was always about 90%-95%. The percentage yield of the corresponding ketone products was calculated using the conversion and the recovered mass of the product. All the conversions for all the reactions have been listed in Table S1 (Supporting Information). For all the oxidations of model compounds, the ^{1}H-NMR spectroscopy showed there were no side reactions occurring, as there were no other products detected except the relevant aldehyde/ketone.

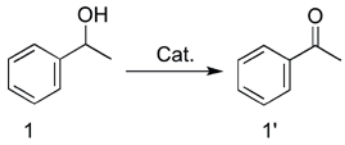

Scheme 1: Screening reaction with 1-phenylethanol.

Table 1: Initial investigation of oxidation of 1-phenylethanol

Entry	Catalyst	Time	Conditions	Yield
1	MnO_2 (10 mmol)	20 h	Ambient	55%
2	MnO_2 (10 mmol)	20 h	40°C, O_2	57%
3	MnO_2 (15 mmol)	20 h	Ambient	71%
4	MnO_2 (5 mmol)	20 h	Ambient	12%
5	MnO_2 (10 mmol)	3 h	UV (λ=254 nm), O_2	92%
6	MnO_2 (10 mmol)	3 h	UV (λ=365 nm), O_2	92%

Note: Petroleum benzine was used as the solvents for all the reactions.

Screening reactions were carried out to test several conditions. Initial reactions were conducted using water as a solvent under ambient conditions, however no reaction was observed. Table 1 shows that the oxidation of 1-phenylethanol occurred when using petroleum benzine as a solvent at ambient conditions with 55% yield.

Increasing the reaction temperature to 40°C and bubbling oxygen through the reaction only marginally increased the yield by 2%. The dosage of MnO_2 was also investigated. Higher MnO_2 dosage could significantly increase the yield from 12% with 5 mmol of MnO_2 to 71% with 15 mmol of MnO_2. When both UV (λ=365 nm) (Table 1, Entry **5**) and UV (λ=254 nm) (Table 1, Entry **6**) irradiation and oxygen were applied for the reaction resulting the yield increased to 92% with 3 hours. The hypothesis is that MnO_2 could absorb photons leading the reduction of Mn (IV) to Mn (II), which resulted in the occurrence of the reaction.[26-30]

Based on the results above, we continued to optimize the conditions for this oxidation reaction. The standard conditions for Table 2 are 10mmol of δ-MnO_2, 1.64 mmol of 1-phenylethanol and oxygen bubbled through, unless otherwise stated. Decreasing the amount of δ-MnO_2 from 10mmol to 5 mmol lead to a drop in yield from 92% (Table 2, Entry 1) to 25% under 365 nm UV (Table 2, Entry 2).

The suggested reason for this occurrence is that due to the heterogeneous nature of the system, the effective concentration of MnO_2 available for the reaction is much lower than the total amount of MnO_2, meaning that a large excess is required. Zhou et al. [41] proved that the photon from wavelength 350 nm to 570 nm could meet the band gap energy of the birnessite, which is a natural form of δ-MnO_2. This, along with the consideration of reducing the health hazards posed by the use of UV light, a blue LED (λ=470 nm) system was tested for the oxidation. The results in Table 2, Entry 4, indicated that the blue light could also efficiently enhance the oxidation reaction, with yield reaching 93% when the reaction was undertaken for 3 hours. ^{1}H-NMR spectroscopy(Fig. S1) and GC-MS (Fig. S2) spectra were shown in supporting information. As such, blue light was selected as the light source for further oxidation reactions. A control reaction involving the amount of MnO_2, but no oxygen bubbled through was also carried out to further elucidate the role of the irradiation of MnO_2 in the reaction.

Table 2: Screening reaction of oxidation of 1-phenylethanol.

Entry	Wavelength	Time	Notes	Yield
1	365 nm	3 h	Standard conditions	92%
2	365 nm	3 h	5 mmol MnO_2	25%
3	470 nm	2 h	10 mmol MnO_2	72%
4	470 nm	3 h	Standard conditions	93%
5	470 nm	3 h	Under air[a]	48%
6	470 nm	3 h	Recycled MnO_2	24%
7	470 nm	3 h	Furnace treated recycled MnO_2	92%

Note:[a] This reaction was performed under air without oxygen bubbled through. [b]Petroleum benzine was used as the solvents for all the reactions.

Table 3: Screening reaction of oxidation of 1-phenylethanol with four types of MnO_2.

Entry	Wavelength	Time	Notes	Yield
1	470 nm	2 h	δ-MnO_2	71%
2	470 nm	2 h	α-MnO_2	28%
3	470 nm	2 h	β-MnO_2	35%
4	470 nm	2 h	γ-MnO_2	25%

Note: Petroleum benzine was used as the solvent for all the reacitons.

The yield of acetophenone after the reaction decreased to 48% (Table 2, Entry 5) and 57% (Table 1, Entry 2) without oxygen bubbled through or blue light respectively. This indicated that both the irradiation and oxygen flow are very important for the regeneration of manganese (II) to manganese (IV) under the irradiation of blue light.

The recyclability of the δ-MnO_2 was tested and only gave a yield of 24% (Table 2, Entry 6) using the recycled MnO_2 without further treatment. The reactivation of δ-MnO_2 was achieved by heating the recovered δ-MnO_2 in a furnace at 230°C for 15 min in air (Table 2, Entry 7). A significant weight loss (13% to 30%) in the catalyst was noted as a result of the furnace reactivation. This weight loss has been previously observed by Arena et al.[33] and was attributed to adsorbed reactants, products and solvent. Thermogravmetic analysis (TGA) was used to analyse the recovered δ-MnO_2 after the reaction. The TGA spectrum has been added in the supporting information as Figure S8. Two weight loss peaks were appeared from TGA and the first weight loss peak was related to the loss of the absorbed solvent (10 to 25% weight loss) while another weight loss peak around 200°C was related to the absorbed substrate/product (3 to 5% weight loss). As a control reaction, MnO_2 was soaked and stirred in the solvent petroleum benzine for 24 h before the reaction. The reaction of oxidation of 1-phenylethanol using this pretreated MnO_2 under the standard condition resulted a yield of 88%, which is slightly lower than the reaction without the solvent pretreatment (93% of yield).

Table 4. δ-MnO_2 oxidation reactions for different alcohol classes.

Substrate	Wavelength	Time	Yield
1-pentanol	470nm	3h	26%
2-pentanol	470nm	3h	0%
Furfuryl alcohol	470nm	3h	69%
Benzyl alcohol	470nm	3h	64%
Cinnamyl alcohol	470nm	3h	92%
Diphenyl ether	470nm	3h	0%
Lignin model compound 1	470nm	3h	89%
Lignin model compounds 2	470nm	3h	90%
Lignin model compounds 3	470nm	3h	89%

Note: Petroleum benzine was used as the solvents for all the reactions.

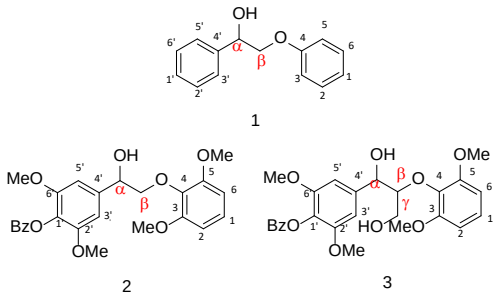

Fig. 5: Lignin model compounds.

All the above results indicated that the solvent has a minor effect and the catalyst deactivation of recovered MnO_2 was mainly due to the adsorption of substrate/product that on the surface. Consequently, these adsorbed substrate/product on the MnO_2 surface inhibit its oxidation efficiency and explains the need to use excess amounts with respect to the substrate in all the reactions. The recycled and reactivated δ-MnO_2 was shown to achieve a quantitative yield to acetophenone (92% yield) when re-used in the oxidation reaction. In addition, there was no MnO_2 solubilised during the process as no MnO_2 or manganese salts were observed after evaporating the filtrate. The structure of the reactive MnO_2 was confirmed by XRD (Fig. S7) showing it was still δ-MnO_2.

Next, four types of manganese dioxide, α-, β-, γ-, and δ-MnO_2 were synthesized by a reported thermo method.[44] Table 3 presents the results of oxidation of 1-phenylethanol using each of the different forms.

The reaction catalysed by δ-MnO_2 showed a yield of 71% with 2 hours reaction time (Table 3, Entry 1), which is a higher yield than was achieved for any other form of MnO_2. This indicated δ-MnO_2 has the highest catalytic ability for oxidizing alcohols of the different forms of MnO_2.

Based on the results of the various optimisation trials, it was decided to use 10 mmol of δ-MnO_2 to 1.64 mmol of substrate with oxygen bubbled through under the irradiation of blue light (λ=470 nm) as the standard condition for further reactions. Some variability in the reactivity of the different alcohol classes was noted in Table 4. A relatively low yield of pentaldehyde (26%) was achieved for the oxidation of 1-pentanol under the standard conditions chosen. Furthermore, 2-pentanol did not give any reaction. "Benzylic" type alcohols (1-phenylethanol, furfuryl alcohol, benzylalcohol) and the one conjugated alcohol (cinnamyl alcohol) in the test compounds all gave good yields of oxidation products. Three β-O-4 lignin model dimers (Fig. 5) were also synthesised to test the reaction, which also showed good yields of oxidation products. All the yields were calculated based on the ^{1}H-NMR spectroscopy. The conversion of lignin model 1 was based on the ratio of signal of protons on the C_β before reaction to after the reaction (Supporting Information Fig. S3).

Table 5. δ-MnO_2 oxidation reactions of 1-phenylethanol with different solvents.

Entry[a]	Solvent	Time	Yield
1	Toluene	2h	72%
2	Chloroform	2h	18%
3	Acetonitrile	2h	64%
4	Petroleum Benzine/ 1 mol equivalent of acetic acid	3h	9.5%

[a] For all the entries, 1-phenylethanol was used as the substrate and the wavelength is 470 nm. [b] Standard reaction conditions were used in all reactions and involved the use of 10mmol of δ-MnO_2, 1.64 mmol of 1-phenylethanol dissolved in the solvent and oxygen bubbled through at ambient temperature (20-23°C), unless otherwise stated.

The conversion of lignin model 2 and 3 were based on the ratio of signal of protons on the C_6 before reaction to after the reaction (Supporting Information Fig. S4). The yields of these three lignin model compounds were calculated by conversion times mass yield.

This showed the potential for lignin oxidation using δ-MnO_2 under mild conditions using blue light. The secondary alcohol in β-O-4 bonds in lignin can be oxidised into ketone bonds, which leads to the bond dissociation energy reduction of the β-O-4 bonds. Thus, oxidised β-O-4 linkages can be cleaved more readily.

Changing the solvent to toluene or acetonitrile did not significantly affect the yield of product for 1-phenylethanol using 2 hours reaction time (Table 5). However, a change to chloroform gave a significant yield loss. Chloroform is known to be slightly acidic.[38] The presence of acid on the reaction was separately tested by adding acetic acid to the reaction mixture. The yield of acetophenone was significantly suppressed (9.5% yield) compared to 93% yield under the same conditions, but without added acid. The effect of the acid, coupled with the order of reactivity of the various alcohols tested, suggests the possible involvement of anionic species in the reaction mechanism.

The reaction mechanism for the oxidation of simple alcohols to aldehydes or ketones via metal oxide catalysts has received limited attention and is not well understood. Arena et al.[38] suggested that the active oxygen species for alcohol oxidation could be either O_2^- or O_2^{2-} based on other studies on manganese oxide octahedral molecular sieves (OMS). Iyer et al.[42] proposed a mechanism for the photo oxidation of 2-propanol to acetone on the surface of a manganese oxide OMS catalyst. Furthermore, Cao and Suib[36] and Duan et al.[37] proposed that the oxygen released from the MnO_2 catalysts is in the form of O_2^- and originates from the movement of this species from the catalyst bulk structure to the surface upon the absorption of light that weakens the MnO_2 bonds. The involvement of lattice oxygen has also been proposed in another study by Makwana et al.[49], involving the oxidation of benzyl alcohol with OMS MnO_2.

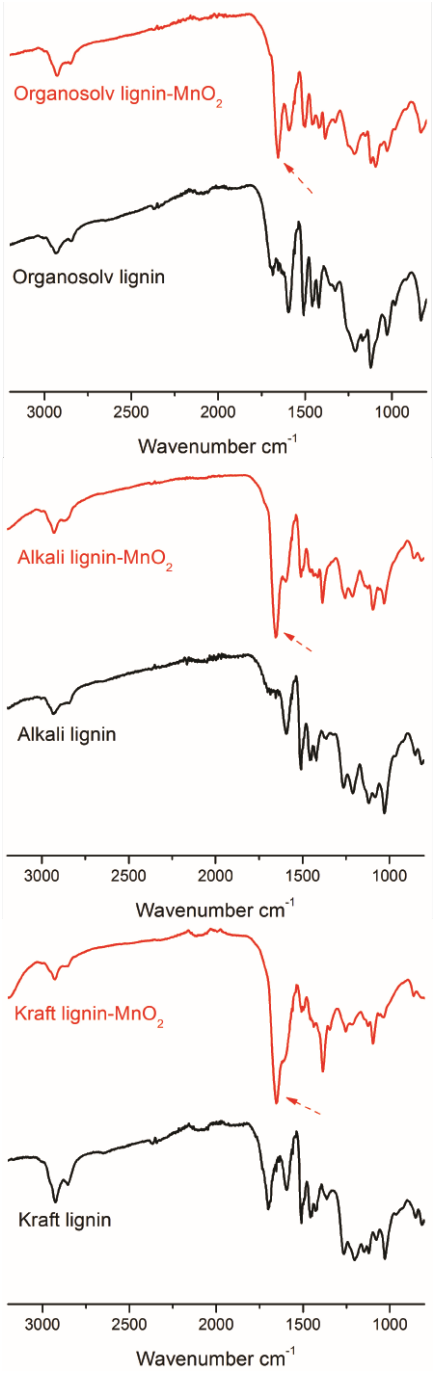

Fig. 6: Infrared Spectra of MnO_2 oxidised lignin samples.

The oxygen species abstracts hydrogen from the alcohol and this abstracted hydrogen (H) is further oxidised to H^+ forming acid sites on the surface of the catalyst.[17] It is conceivable that the O_2^- species on the surface of the catalyst would be suppressed by the presence of acid in the reaction medium. Gas phase oxygen from air, which is bubbled through the reaction medium, then acts to reoxidise the manganese (II) to the manganese (IV).[36-37]

The results of oxidation for the lignin model compounds in Table 4, indicates that this strategy showed high potential for the oxidation of lignin itself.

Oxidation reactions of lignins

For these oxidation trials, three lignin sources were utilized; organosolv lignin, kraft lignin, and alkali lignin. All three lignin samples were analysed by 2D-NMR to give structural information, shown in Fig. 7 (a), (b), and (c). Three typical bonds, β-O-4 bonds, β-β bonds, and β-5 bonds were detected, and are shown in Fig. 7. The full HSQC-NMR spectra with integration (Fig. S9, Fig. S10, Fig. S11) and the content of β-O-4 bonds in the three lignin samples are listed (Table S2 and Table S3) in the supporting information.

After characterisation of the lignin samples, δ-MnO_2 photo-catalytic oxidations were carried out. The reaction mixture is not fully homogeneous due to the solubility of lignin in acetonitrile. The optimized conditions (200 mg of lignin, 10 ml of acetonitrile, and 870 mg of MnO_2, 3 hours with oxygen bubbled through under the irradiation of blue light) were applied to all these three samples.

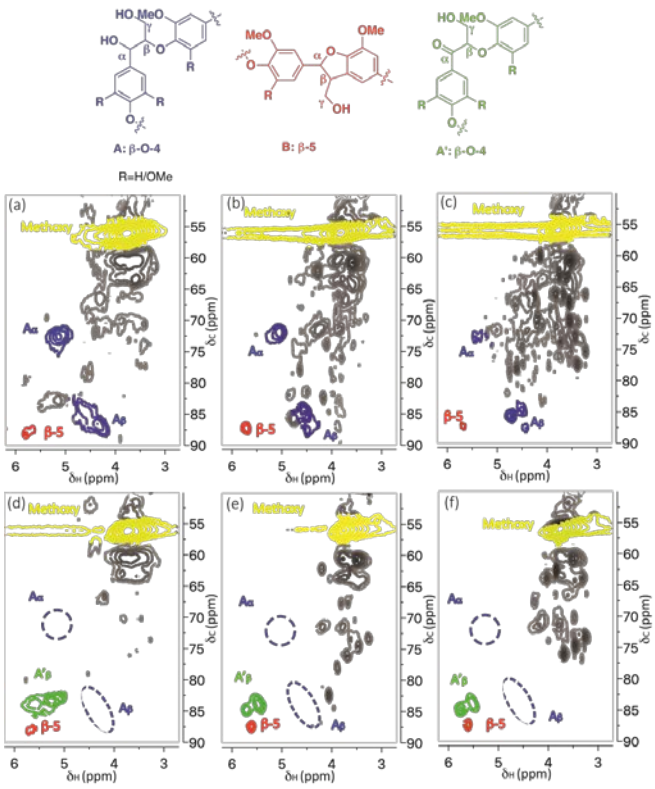

Fig. 7: Different lignin linkages and 2D-NMR spectra of (a) organosolv lignin, (b) alkali lignin, (c) kraft lignin, (d) oxidised organosolv lignin, (e) oxidised alkali lignin, and (f) oxidised kraft lignin.

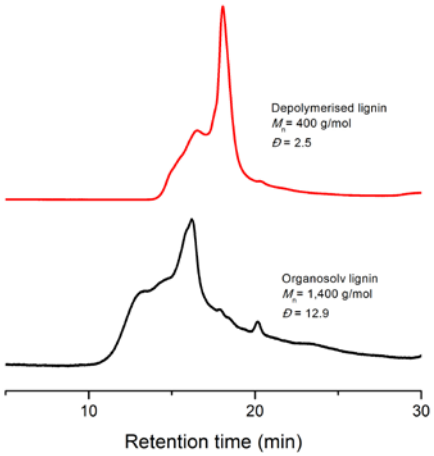

Fig. 8: SEC chromatograms of depolymerised lignin ethyl-acetate soluble fraction

The products were analysed by IR to determine the presence of newly introduced carbonyl frequencies, as evidence of oxidation having occurred.[50-52] The results of this IR analysis are shown in Fig. 6. The black curves are the samples before oxidation and the red curves are the samples after oxidation. After oxidation, new peaks around 1700 cm^{-1} appeared (labelled with arrows), which are peaks typical of C=O bonded to an aromatic ring.[51-53] This demonstrated that all these lignin samples were successfully oxidised with δ-MnO_2 as a photo-catalyst.

Oxidised lignin samples were also analysed by 2D-NMR to give further structural information. 2D-NMR spectra of oxidised lignin are shown in Fig. 7 (d), (e), and (f), which support the finding that β-O-4 bonds were oxidised in the lignin during this process. When comparing lignin before the reaction Fig. 7(a), (b), and (c) to after the reaction Fig. 7(d), (e), and (f), the signal from A_α disappeared after oxidation. This suggested the secondary hydroxyl group at the C_α position was oxidised to a ketone. In addition, the signal of A_β shifted after oxidation. This indicated the β-O-4 bonds were successfully oxidised without bond cleavage. In addition, the signal from β-5 bonds still existed after oxidation. The percentages of β-O-4 bonds before and after oxidation have been listed in Table S2 (Supporting Information). A previously reported method was used to calculate the ratio of linkages.[18,55]

After oxidation, a depolymerisation strategy that has been previously reported was applied for lignin depolymerisation. Formic ionic liquid, [54] 2-hydroxy ethylammonium formate, was used for the depolymerisation of oxidised lignin. The proposed mechanism has been reported[54] as the bond dissociation energy of C_β-OPh decreased after oxidation. The formate anion will attack the other hydroxyl group in the oxidised β-O-4 bonds resulting in C_β-O bond cleavage.

After the reaction, ethyl acetate was used to extract the low molecular weight fraction of the product mixture. SEC was used to analyse the molecular weight before (black curve) and after (red curve) depolymerisation reactions (Fig. 8). Oxidised lignin was successfully depolymerised with the generation of ethyl acetate fraction yielding 51% of soluble products, increased from 12% prior to reaction. The molecular weight decreased from M_n = 1,400 to M_n = 400 with polydispersity decreased from 12.9 to 2.5 (Fig. 8). This indicated that the oxidised organosolv lignin was successfully depolymerised with the molecular weight decreased. The signal in the red curve from the retention time around 18 min significantly increased compared to the black curve. This indicated there was a significant generation of low molecular weight fractions after depolymerisation. The GC-MS spectrum (Fig. S13) of ethyl-acetate soluble fraction from the depolymerised organosolv lignin showed that monomers including 4-hydroxy-3,5-dimethoxybenzaldehyde, and oligomers were produced after depolymerisation. However, these products were difficult to isolate from the mixture.

Conclusions

In this study, we presented a novel heterogeneous photo-catalytic system to oxidise lignin using recyclable MnO_2 at ambient temperature. Blue light, was used as the light source instead of UV light or any other conventional heating. Several solvents were tested and found that acetonitrile can be used for the lignin oxidation. Three different lignin samples were successfully and efficiently oxidised and shown that they can be partially depolymerised. The amount of MnO_2 requires for the oxidation of phenols and lignin is still high (ca. 5-hold) and requires heat 230°C for 15 min to recycle MnO_2 and needs further study to improve the catalytic activity of MnO_2 by controlling its surface area and pore size in the future.

Experimental

Material:

Organosolv lignin (M_n = 1,400 g/mol, $Đ$ = 12.9 by SEC) from corn cob from *Stigmate maydis* was purchased from Chemical Point (Munich, Germany). Kraft lignin (M_n= 1,500 g/mol, $Đ$=7.7 by SEC) was isolated through the process described later from black liquor supplied by Visy from its paper mill in Tumut, NSW, Australia, which mainly uses *Pinus radiata* (softwood). Alkali lignin (M_n = 1,100 g/mol, $Đ$ = 9.1 by SEC) was purchased from Sigma-Aldrich (Sydney, NSW, Australia). All these three lignin samples were used without any further purification. $MnSO_4{\cdot}H_2O$ and $KMnO_4$ were purchased from Sigma-Aldrich. Ethyl acetate, acetonitrile, dimethyl formamide (DMF), chloroform ($CDCl_3$), dimethyl sulfoxide (DMSO-d_6), and methanol were purchased from Merck. All reagents were used as purchased from the supplier without any further purification.

Instruments and measurements:

^{1}H-NMR and 2D-NMR spectroscopy were recorded on a Bruker DRK-600 spectrometer operating at 600 MHz as solutions in $CDCl_3$ and DMSO-d_6. The molecular weight of isolated lignin and depolymerised samples were measured by SEC performed on a Tosoh EcosHLC-8320 Gel Permeation Chromatograph

equipped with both refractive index (RI) and ultraviolet (UV) detectors (UV detection, λ = 280 nm) using Tosoh alpha 4000 and 2000 columns. DMF (with 10 mM LiBr) was used as solvent to dissolve all the lignin samples as well as mobile phase with flow rate of 1.0mL/min. UV detector in SEC chromatograms set at 280 nm was used to analyse all the depolymerised samples and isolated lignin. Calibration curves were obtained using polystyrene standards. The SR-02-B0040 LED assembly has 7 LXML-PB01-0040 Blue (470 nm) LUXEON Rebel LEDs soldered to a 40 mm round 7-Up CoolBase and run with 40V and a 1000 mA current draw. UV irradiations were performed using a CL1000 M UV-crosslinker lamp (UVP, LLC, Australia) that provide polychromatic light centred at 365nm and 254 nm. The N_2-physical adsorption isotherms (77K) were obtained using an ASAP 2010 static adsorption device (Micromeritics Instrument). Before measurement the sample was outgassed at 150°C for 6h. Surface area (SA), pore volume (PV) and average diameter (APD) data were obtained from the elaboration of the isotherm by the standard BET and BJH methods, respectively. X-ray diffraction (XRD) analyses were performed using a Philips X-Pert diffractometer, operating with Ni β-filtered Cu Kα radiation (40 kV; 30 mA) at a scan rate of 0.05°/min. Temperature programmed reduction (H_2-TPR) measurements in the range of 293-1073K were carried out using a linear quartz microreactor (dint=4 mm) heated at the rate of 12K/min. The reactor was loaded with a catalyst sample of ca. 20 mg and fed with a 5% H_2/Ar carrier (F, 60 stpmL/min). The H_2 consumption was monitored by a TCD, after water removal by a "chemical trap" containing $Mn(ClO_4)_2$.

Isolation of kraft lignin from black liquor:

The procedure to isolate kraft lignin from black liquor has been reported before.[51-52,54] Elemental analysis of carbon, hydrogen, nitrogen and sulphur gave the following result (average over three measurement): Carbon 65.30%, Hydrogen 6.07%, Nitrogen <0.3% (detection limit), Sulphur 2.57%. M_n= 1,500 g/mol, $Đ$=7.7

Synthesis of δ-MnO_2:

A 100 mL round bottom flask was filled with 70 ml of distilled water and stir bar. $MnSO_4 \cdot H_2O$ (1.69 g, 1 mol) and $KMnO_4$ (1.58 g, 1 mol) were added into the round bottom flask. The mixture was stirred for 2 hours at the temperature of 80°C. After 2 hours, 0.5 g of NaOH was added into the mixture and was stirred for another 2 hours. After reaction, the brown residue, which is MnO_2, was filtered and washed with distilled water to remove all the unreacted chemicals. The filter cake was then dried in the oven at the temperature of 100°C for over night. Power XRD was used to confirm the structure of the MnO_2.

Procedure for oxidation of 1-phenylethanol with MnO_2:

A 100 mL round bottom flask was charged with 0.2 ml (d = 1.013 gmL^{-1}, 202 mg, 1.64 mmol) of 1-phenyl ethanol and 10 ml of petroleum benzine. MnO_2 was then added to the desired quantity (eg. 870 mg, 10 mmol) and the solution stirred vigorously at room temperature for 20 hours. After the reaction, MnO_2 was removed by filtration. The mixture was then partitioned between water (30 mL) and ethyl acetate (2 x 20 mL). The combined organic layers were washed with saturated brine (1 x 30 mL) and dried over anhydrous magnesium sulfate. The solvent was removed in *vacuo* and the product was then analysed by ^{1}H-NMR to determine the percentage yield of the secondary alcohol to a ketone. **^{1}H NMR** (400MHz, $CDCl_3$), 7.94 (δ, J = 7.6Hz, 2H), 7.48 (m, 3H), 2.58 (s, 3H).

Procedure for UV (365nm) oxidation of 1-phenylethanol with MnO_2:

A UV reactor was charged with 0.2 ml (d = 1.013 gmL^{-1}, 202 mg, 1.64 mmol) of 1-phenyl ethanol and 10 ml of petroleum benzine. 870 mg, 10 mmol of MnO_2 was then added to the mixture. A UV light was suspended in the reactor, and oxygen bubbled through the solution. The reactor was then covered in foil and stirred without external heating for 5 hours. After the reaction, MnO_2 was recovered by filtration. The mixture was then partitioned between water (30 mL) and ethyl acetate (2 x 20 mL). The combined organic layers were washed with saturated brine (1 x 20 mL) and dried over anhydrous magnesium sulfate. The solvent was removed *in vacuo* and the product was then analysed by ^{1}H-NMR to determine the percentage yield of the secondary alcohol to a ketone.

Procedure for 470nm oxidation of 1-phenylethanol with MnO_2:

A 100 mL round bottom flask was charged with 0.2 ml (d = 1.013 gmL^{-1}, 202 mg, 1.64 mmol) of 1-phenyl ethanol and 10 ml of petroleum benzine. Manganese dioxide was then added (870 mg, 10mmol) and the solution stirred vigorously at room temperature for 3 hours under irradiation with 470nm blue light. The mixture was then partitioned between water (30 mL) and ethyl acetate (2 x 20 mL). The combined organic layers were washed with saturated brine (1 x 30 mL) and dried over anhydrous magnesium sulfate. The solvent was removed *in vacuo* and the product was then analysed by ^{1}H-NMR to determine the percentage yield of the secondary alcohol to a ketone

Procedure for 365nm/254nm oxidation of 1-phenylethanol with δ-MnO_2:

A 100 mL round bottom flask was charged with 0.2 ml (d = 1.013 gmL^{-1}, 202 mg, 1.64 mmol) of 1-phenyl ethanol and 10 ml of petroleum benzine. MnO_2 was then added (870 mg, 10mmol) and the solution stirred vigorously at room temperature for 3 hours in a CL1000 M UV-crosslinker under irradiation with 365 nm or 254 nm lamps. The mixture was then partitioned between water (30 mL) and ethyl acetate (2 x 20 mL). The combined organic layers were washed with saturated brine (1 x 30 mL) and dried over anhydrous magnesium sulfate. The solvent was removed *in vacuo* and the product was then analysed by ^{1}H-NMR to determine the percentage yield of the secondary alcohol to a ketone.

Procedure for 470nm Oxidation of Lignin with MnO_2:

A 100 mL round bottom flask was charged with 200 mg of lignin and 10 ml of acetonitrile. 870 mg (10mmol) of MnO_2 was then added and the solution stirred vigorously at room temperature for 3 hours under irradiation with 470 nm blue lights. The mixture was then diluted (using methanol for methanol soluble lignin, and DMF for methanol insoluble) and the MnO_2 filtered off. The solvent was removed *in vacuo* and the product was then analysed by FTIR and SEC.

Synthesis of 2-phenoxy-1-phenylethanol (lignin model 1):

A 250 ml round bottom flask was equipped with a reflux condenser and dropping funnel was charged with phenol (0.520 g, 5.53 mmol) and stirred at room temperature. To this solution, 2-bromoacetophenone (1.00 g, 5.02 mmol) in acetone (50 ml) was added dropwise over 30 min at room temperature. The resulting suspension was stirred at reflux for 4 hours, after which the suspension was filtered and concentrated in vacuum. The crude product was purified by recrystallisation from ethanol to give 2-phenoxy-1-phenylethanone as white solid (1.050 g, 4.95 mmol) in 98% yield. To a solution of 2-phenoxy-1-phenylethanone (0.315 g, 1.49 mmol) in ethanol, $NaBH_4$ (0.112 g, 2.98 mmol) was added at 0°C. The resulting solution was stirred at 0°C for 5 min. The reaction mixture was partitioned between ethyl acetate (50 ml) and water (30 ml). The organic layer was washed with saturated brine (30 ml, twice), dried over Na_2SO_4 and evaporated under reduced pressure to give 2-phenoxy-1-phenylethanol as a white solid (0.301 g in 94% yield). ^{1}H-NMR: 400 MHz, $CDCl_3$) δ 7.45 (d, 2H), 7.38 (t, 2H), 7.33 (d, 1H), 7.27 (t, 2H), 6.96 (t, 1H), 6.91 (d, 2H), 5.12 (dt, 1H), 4.10 (dd, 1H), 3.99 (t, 1H), 2.76 (d, 1H) ESI: m/z 214.1, found 214.0.

Synthesis of lignin model 2:

1-(4-Benzoyloxy-3,5-dimethoxyphenyl)-2-(2,6-dimethoxyphenoxy)ethanone was synthesized following a reported procedure.[56] ^{1}H-NMR: 400 MHz, $CDCl_3$) δ 8.5 (d, 1H), 8.13 (m, 2H), 7.60 (tt, 3H), 6.97 (t, 1H), 6.85 (ds, 2H), 6.75 (d, 2H), 5.17 (m, 2H), 4.60 (m, 1H), 4.40 (m, 1H), 3.9 (s, 6H). 3.8 (s, 6H).ESI: m/z: 454.16, found 454.0.

Synthesis of lignin model 3:

The synthesis of lignin model 3 was following a reported procedure.[56] The ^{1}H-NMR: ^{1}H-NMR: 400 MHz, $CDCl_3$) δ 8.9 (t, 1H), 8.5 (d, 1H), 8.13 (m, 2H), 7.60 (tt, 3H), 6.97 (t, 1H), 6.85 (d, 2H), 6.72 (d, 2H), 5.04 (m, 2H), 4.25 (m, 1H), 4.00 (m, 1H), 3.9 (s, 6H). 3.83 (m, 1H), 3.8 (s, 6H).ESI: m/z: 486.17, found 486.0.

Procedure for Oxidised Lignin Depolymerisation in Formic Ionic Liquid (2-hydroxy ethylammonium formate):

A 100 mL round bottom flask was charged with 200 mg of lignin and 10 ml of synthesized formic ionic liquid. The synthesis of this ionic liquid has been previously reported.[57] The mixture was then heated at 110°C for 24 h. After the reaction, the ionic liquid was distilled at the temperature of 120°C at 0.4 mbar. The residue was then extracted with ethyl acetate and water. Ethyl acetate was removed from the organic layer under vacuum to give low molecular weight fraction. Products were analysed by SEC.

Synthesis of α-, β-, γ-, and δ-Manganese Dioxide Catalysts:

The procedures used followed reported methods.[44] In a typical synthesis of the α-MnO_2 nanorods, 2.5 g of $KMnO_4$ and 1.05 g of $MnSO_4{\cdot}H_2O$ were mixed in distilled water (160 mL) and magnetically stirred about 10 min to form a homogeneous mixture. Then, the mixture was transferred into a Teflon-lined stainless steel autoclave (400 mL) and heated at 160 °C for 12 h. The product was collected, washed, and dried at 80 °C. Similarly, the β-MnO_2 nanorods were obtained from the reaction of $KMnO_4$ (1.40 g) and $MnSO_4{\cdot}H_2O$ (2.25 g) at 160 °C for 12 h. For the preparation of the *γ*-MnO_2 nanorods, $MnSO_4{\cdot}H_2O$ (6.75 g) and $(NH_4)_2S_2O_8$ (9.15 g) were well mixed and hydrothermally treated at 90 °C for 24 h. The *δ*-MnO_2 nanorods were obtained by the chemical oxidation of $MnSO_4{\cdot}H_2O$ (0.55 g) and $KMnO_4$ (3 g), which were hydrothermally heated at 240°C for 24 h. All the catalysts were analyzed by Powder XRD to confirm the structures.

Conflicts of interest

There are no conflicts to declare.

Acknowledgements

This work is dedicated to the memory of the late Professor Leone Spiccia whose work on the application of manganese catalysts for water splitting under UV and visible light irradiation inspired this study.

The financial support of the ARC Industrial Transformation Research Hub - Bioprocessing Advanced Manufacturing Initiative (BAMI), Monash University, PRESTO JST, JPMJPR1515, Japan and the China Scholarship Council (CSC) is gratefully acknowledged.

References

1 J. Zakzeski, P. C. A. Bruijnincx, A. L. Jongerius, B. M. Weckhuysen, *Chem. Rev.* 2010, **110**, 3552-3557.
2 C. Xu, R. A. D. Arancon, J. Labidi, R. Luque, *Chem. Soc. Rev.* 2014, **43**, 7485-7500.
3 B. M. Upton, A. M. Kasko, *Chem. Rev.* 2015**, 116**, 2275-2306.
4 Z. Jiang, C. Hu, *J. Energy Chem.* 2016, **25**, 947-956.
5 J. Dai, A. F. Patti, K. Saito, *Tetrahedron Lett.* 2016, **57**, 4945-4951.
6 P. Azadi, O. R. Inderwildi, R. Farnood, D. A. Kin, *Renewable and Sustainable Energy Rev.* 2012, **21**, 506-523.
7 F. S. Chakar, A. J. Ragauskas, *Ind. Crops Prod.* 2004, **20**, 131-141.
8 P. Azadi, O. R. Inderwildi, R. Farnood, D. A. King, *Renewable and Sustainable Energy Rev.* 2013, **21**, 506-523.
9 P. J. Deuss, K. Barta, *Coord. Chem. Rev.* 2016, **306**, 510-532.

10 S. Kim, S. C. Chmely, M. R. Nimlos, Y. J. Bomble, T. D. Foust, R. S. Paton, G. T. Beckham, *J. Phys. Chem. Lett.* 2011, **2**, 2846-2852
11 P. J. Deuss, C. S. Lancefield, J. G. de Vries, N. J. Westwood, K. Barta, *Green Chem.* 2017, **19**, 27774-2782.
12 S. Constant, H. L. Wienk, A. E. Frissen, P. de Peinder, R. Boelens, D. S. Van Es, R. J. Grisel, B. M. Weckhuysen, W. J. Huijgen, R. J. Gosselink, *Green Chem.*, 2016, **18**, 2651-2665.
13 C. Crestini, H. Lange, M. Sette, D. S. Argyropoulos, *Green Chem.*, 2017, **19**, 4104-4121.
14 A. Das, A. Rahimi, A. Ulbrich, M. Alherech, A. H. Motagamwala, A. Bhalla, L. da Costa Sousa, V. Balan, J. A. Dumesic, E. L. Hegg, *ACS Sustainable Chem. Eng.*, 2018, **6**, 3367-3374.
15 I. Bosque, G. Magallanes, M. Rigoulet, M. D. Kärkäs, C. R. Stephenson, *ACS Cent. Sci.*, 2017, **3**, 621-628.
16 A. Rahimi, A. Ulbrich, J. J. Coon, S. S. Stahl, *Nature* 2014, **515**, 249-252.
17 Y. Yang, H. Fan, Q. Meng, Z. Zhang, G. Yang, B. Han, *Chem. Commun.* 2017, **53**, 8850-8853.
18 C. S. Lancefield, O. S. Ojo, F. Tran, N. J. Westwood, *Angew. Chem.* 2015, **127**, 260-264.
19 O. Lanzalunga, M. Bietti, *J. Photochem. Photobiol., B* 2000, **56**, 85-108.
20 C. M. Teh, A. R. Mohamed, *J. Alloy. Compd.* 2011, **509**, 1648-1660.
21 S.-H. Li, S. Liu, J. C. Colmenares, Y.-J. Xu, *Green Chem.* 2016, **18**, 594-607.
22 J. C. Colmenares, R. Luque, *Chem. Soc. Rev.* 2014, **43**, 765-778.
23 A. Fujishima, K. Honda, *Nature* 1972, **238**, 37-38.
24 S. G. Kumar, L. G. Devi, *J. Phys. Chem. A* 2011, **115**, 13211-13241.
25 V. Molinari, C. Giordano, M. Antonietti, D. Esposito, *J. Am. Chem. Soc.* 2014, **136**, 1758-1761.
26 W. Li, M. Zhang, Z. Du, Q. Ma, H. Jameel, H.-m. Chang, *BioResources* 2015, **10**, 1245-1259.
27 J. D. Nguyen, B. S. Matsuura, C. R. Stephenson, *J. Am. Chem. Soc.* 2014, **136**, 1218-1221.
28 K. Tanaka, R. Calanag, T. Hisanaga, *J. Mol. Catal. A: Chem.* 1999, **138**, 287-294.
29 M. Ksibi, S. B. Amor, S. Cherif, E. Elaloui, A. Houas, M. Elaloui, *J. Photochem. Photobiol., A* 2003, **154**, 211-218.
30 A. E. Machado, A. M. Furuyama, S. Z. Falone, R. Ruggiero, D. da Silva Perez, A. Castellan, *Chemosphere* 2000, **40**, 115-124.
31 M. M. Najafpour, M. Fekete, D. J. Sedigh, E. M. Aro, R. Carpentier, J. J. Eaton-Rye, H. Nishihara, J. Shen, S. I. Allakhverdiev, L. Spiccia, *ACS Catal.*, 2015, **5** (3), 1499–1512.
32 G. W. Brudvig, N. H. Reek, K. Sakai, L. Spiccia, L. Sun, *ChemPlusChem*, 2016, **81** (10), 1017-1019.
33 J. Joy, J. Mathew, S. C. George *Int. J. Hydrogen Energy* 2018**, 43**, 4804-4817.
34 A. P. Black, H. Suzuki,b, M. Higashi, C. Frontera, C. Ritter, C. De, A. Sundaresan, R. Abe, A. Fuertes, *Chem. Commun*, 2018, **54**, 1525-1528.
35 S. Chen, T. Takata, K. Domen, *Nat. Rev. Maters.* 2017, **(2)** 17050.
36 H. Cao and S. L..Suib, *J. Am. Chem. Soc*. 1994, **116**, 5334-5342.
37 L. Duan, B.Sun, M.Wei, S.Luo, F.Pan, A.Xu, X.Li, *J. Hazard. Mater.*, 2015, **285**, 356–365.
38 F. Arena, B. Gumina, A. F. Lombardo, C. Espro, A.F. Patti, L. Spadaro, L. Spiccia, *Appl. Catal. B: Environ*. 2015**, 162**, 260-267.
39 R. Xu, X. Wang, D. Wang, K. Zhou, Y. Li, J. Catal., 2006, **237**, 426-430.
40 J.C. Hunter, *J. Solid State Chem.*, 1981, **39**, 142-147.
41 R. J. Gritter, T. J. Wallace, *J. Org. Chem.* 1959, **24**, 1051-1056.
42 F. Zhou, A. Izgorodin, R. K. Hocking, V. Armel , L. Spiccia, D. R. Macfarlane, *J. Mater. Chem. A*, 2015, **3**, 16642-16652.
43 F. Zhou, A. Izgorodin, R. K. Hocking, V. Armel, L. Spiccia, D. R. MacFarlane, *ChemSusChem* 2013, **6**, 643-651.
44 F. Zhou, A. Izgorodin, R. K. Hocking, L. Spiccia, D. R. MacFarlane, *Adv. Energy Mater.* 2012, **2**, 1013-1021.
45 S. Liang, F. Teng, G. Bulgan, R. Zong, Y. Zhu, *J. Phys. Chem. C* 2008, **112**, 5307-5315.
46 M. Villalobos, B. Toner, J. Bargar, G. Sposito, *Acta*, 2003, **67**(14), 2649-2662.
47 A. Iyer, H. Galindo, S. Sithambaram, C. King'ondu, C-H. Chen, S. L. Suib. *Appl. Catal., A*, 2010, **375**, 295–302.
48 X. Tang, J. Li, J. Hao*, Catal. Commun*. 2010, **11**, 871–875.
49 V. D. Makwana, Y-C. Son, A. R. Howell, S. L. Suib, *J. Catal.,* 2002, **210**, 46–52.
50 J. Dai, S. Nanayakkara, T. C. Lamb, A. J. Clark, S.-X. Guo, J. Zhang, A. F. Patti, K. Saito, *New J. Chem.* 2016, **40**, 3511-3519.
51 J. Dai, G. N. Styles, A. F. Patti, K. Saito, *ACS Omega*, 2018, **3**, 10433-10441.
52 C. G. Boeriu, D. Bravo, R. J. Gosselink, J. E. van Dam, *Ind. Crops Prod.*, 2004, **20**, 205-218.
53 A.-A. M. Nada, M. Yousef, K. Shaffei, A. Salah, Polym. Degrad. Stab., 1998, **62**, 157-163.
54 J. Dai, A. Patti, L. Longé, G. Garnier, K. Saito, *ChemCatChem*. 2017, **14,** 2684-2690.
55 L. F. Longe, J. Couvreur, M. L. Grandchamp, G. Garnier, F. Allais, K. Saito, *ACS Sustainable Chem. Eng.* 2018, **6**(8), 10097-10107.
56 S. Kawai, K. Okita, K. Sugishita, A. Tanaka, H. Ohashi, *J. Wood Sci.* 1999, **45**, 440-443.
57 N. Bicak, *J. Mol. Liq.*, 2005, **116**(1), 15-18.